

This document is the unedited Author's version of a Submitted Work that was subsequently accepted for publication in Inorganic Chemistry, copyright © American Chemical Society after peer review. To access the final edited and published work see <https://doi.org/10.1021/acs.inorgchem.6b02067>.

Access to this work was provided by the University of Maryland, Baltimore County (UMBC) ScholarWorks@UMBC digital repository on the Maryland Shared Open Access (MD-SOAR) platform.

Please provide feedback

Please support the ScholarWorks@UMBC repository by emailing scholarworks-group@umbc.edu and telling us what having access to this work means to you and why it's important to you. Thank you.

pH surface control of Ag₄₄(MNBA)₃₀ nanoclusters: An approach for tunable optical and electronic properties

Lina G. AbdulHalim^a, Xin Zhang,^b Manas R. Parida^a, Shawkat M. Aly^a, Matthew Pelton^c, Yaroslav Losovyj^d, Peter A. Dowben,^b Osman M Bakr^a, Omar F. Mohammed^{a*} and Khabiboulakh Katsiev^{a*}

^aKing Abdullah University of Science and Technology (KAUST), Physical Sciences and Engineering Division, Solar and Photovoltaics Engineering Research Center (SPERC), Thuwal 23955-6900, Saudi Arabia, ^bDepartment of Physics and Astronomy, University of Nebraska—Lincoln, Lincoln, Nebraska 68588, United States, ^cDepartment of Physics, University of Maryland, Baltimore County, 1000 Hilltop Circle, Baltimore, Maryland 21250, United States, ^dDepartment of Chemistry, Indiana University, Bloomington, IN 47405, USA

KEYWORDS. nanoclusters, transient absorption spectroscopy, tunable optical properties, charge separation

ABSTRACT: Noble metal nanoclusters (NCs) play a pivotal role in bridging the gap between molecules and nanocrystals. Fundamental understanding of the evolution of structural, optical and electronic properties of these materials in various environments is of paramount importance for functional applications. Here we show experimentally how to tune the optical and electronic properties of the most featured Ag₄₄(MNBA)₃₀ NCs by controlling the pH of the solution. Finally, the infrared and photoemission spectroscopies indicate dimerisation between two adjacent ligands capping the NCs takes place upon lowering the pH from 13 to 7.

Introduction

Surface engineering is a unique approach in generating stable, multifunctional and highly ordered nano-structured materials. Ligand modification lies at the forefront of post-synthetic surface engineering tools for rendering the nanoscale materials soluble in a desired solvent and ultimately suitable for particular applications.¹⁻⁴ For instance, to improve transport properties of the quantum dots, initial, capping ligands are exchanged with shorter, conducting molecules.⁵⁻⁸ Another approach employs interfacing nanoscale materials with functional systems such as proteins,⁹ porphyrins¹⁰ or cyclodextrins¹¹ via supramolecular chemistry. On the other hand, atomically precise noble metal nanoclusters (NCs), as a new class of nanoparticles that consist of few tens of atoms (2 nm in size) capped by organic ligands, have also been engineered.¹²⁻¹⁴ These compounds possess unique physicochemical properties, intriguing geometrical structures and quantized charging behaviors.¹⁵⁻¹⁸ The more microscopic interactions governing the structure, dynamics and orderliness of this class of materials need to be explored, however, in order to deploy them in functional devices.^{19, 20}

Similar to the case of semiconductors, quantum size effects, so-called quantum confinement,^{21, 22} the

optical and electronic properties of the NCs can be controlled.²³ This approach fuelled significant progress in the synthesis of NCs of various sizes and compositions. However, the quantum size effect approach is oversimplified because it disregards the impact of *surface/ligands* engineering which is a very effective approach of tailoring the optical and electronic properties of NCs.²⁴⁻²⁸ At such small length scale (less than 2 nm), nearly 30-70% of the atoms reside on the surface. Thus, the chemistry of organic ligands, the surface structure of the NCs and its effect on the electronic properties are of great importance for the applications based on these clusters. Theoretical work and various spectroscopic and microscopic studies on self-assembled monolayers-covered planar Au and Ag single crystal surfaces indicate that the alignment of the molecular states relative to the metal Fermi level and the work function can be tuned by changing the docking chemistry.²⁹⁻³² The choices of the docking chemistry and head-group substitution allow for an independent optimization of ligand-core interfacial properties leading to more stable and better performing NCs.

Although the impact of the ligand orientation on the electronic properties for these type of materials has been reported earlier, few studies have examined the effect of ligand configuration.³³ Herein we report a new strategy of tailoring the optical and

electronic properties of monodisperse thiol-protected silver $\text{Ag}_{44}(\text{MNBA})_{30}$ NCs, (MNBA = 5 mercapto-2-nitrobenzoic acid) via protonation/deprotonation of the ligand shell. In addition, we present the first experimental evidence for the dimerization of the ligand shell through C-H...O interactions upon lowering the pH from 13 to 7 as shown in Scheme 1.

Results and Discussion

The MNBA ligand is composed of benzene ring with a nitro and carboxylate functional groups. It is well documented that the purified NCs are stable for prolonged periods of time in aqueous solutions of high pH (>13).³⁴ At such high pH, all carboxylate groups of the ligands are deprotonated and the NCs are readily soluble in aqueous solutions. Red curve in Figure 1 shows the UV-Vis absorption spectrum of deprotonated $\text{Ag}_{44}(\text{MNBA})_{30}$ NCs.

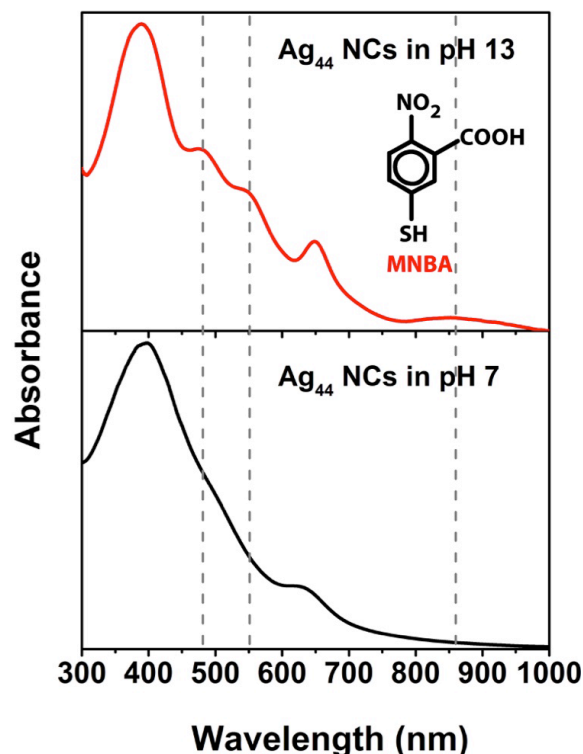
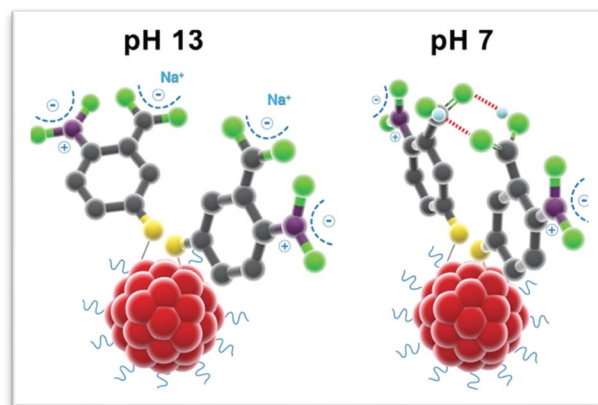


Figure 1. UV-Vis absorption spectra of Ag_{44} NCs in aqueous solutions at different pH. Inset in upper panel shows schematic of the capping ligands.

To protonate the ligands capping the NCs, a concentrated solution of the NCs was diluted with MilliQ water at pH 5.8, and was immediately filtered with Millipore Amicon centrifuge membrane filters centrifuged at 5000 rpm for 30 min. This process was repeated at least 5 times, where each time the filtered NCs were diluted with MilliQ water, to

ensure the protonation of the majority of the ligands. The pH of the final solution is 7 and the corresponding UV-Vis spectrum is displayed in Figure 1 (black curve). Comparing the two spectra at pH 13 and 7, we observe substantial changes in the optical absorption: at lower pH, the peak at 392 nm is broadened whereby no clear transitions appear at 483 or 553 nm. Additionally, the peak at 652 nm is blue shifted by 27 nm and most importantly the peak at 857 nm vanishes completely, turning the solution from bold ruby red to faint yellow. Interestingly, the optical absorption and the color of the NCs are recovered (Figure S1) when the pH is raised again by adding aliquots of 1M sodium hydroxide solution.



Scheme 1. Cartoon of $\text{Ag}_{44}(\text{MNBA})_{30}$ NCs in different pH: Left in pH 13 where the NCs are completely deprotonated, and right in pH 7 where the NCs are protonated and dimerization takes place.

As is well established, the changes in absorption spectra of molecular metal NCs are related to changes in the underlying geometries.³⁵ In this case, we suspect that a structural change of the organic ligand is involved. We suggest that protonation may cause dimerization of the adjacent carboxyl groups as depicted in Scheme 1. A similar phenomenon was recently reported by Gell *et al.* on Ag_{44} NCs using 4-mercaptobenzoic acid as stabilizing ligand.³⁶ They simulated the absorption spectra of the NCs at different pH values, and concluded that dimer interactions on the surface of the NCs were responsible for the observed dimerization. As discussed in the following paragraphs, dimerization alters electronic structure of NCs, which in turn affects electronic transitions.

Since vibrational spectroscopy is informative tool to investigate such possibility of benzoic acid dimer formation^{37, 38} we used FTIR spectroscopy to obtain information about specific interaction between

functional groups, with the particular focus on the C=O stretching vibration to probe any local interaction of the organic ligands including dimerization. The steady-state IR spectra in Figure 2 shows that the C=O stretch vibration for pure ligands is located at 1695 cm^{-1} . For $\text{Ag}_{44}(\text{MNBA})_{30}$ NCs powder prepared from aqueous solution, this value is downshifted to 1583 cm^{-1} pointing to the formation of dimers upon protonation of the NCs; on the other hand, for those prepared from deuterated aqueous solution, the C=O band is upshifted by approximately 13 cm^{-1} compared to the one prepared from normal aqueous solution, providing clear experimental evidence for the involvement of the hydrogen bonding interaction³⁹ between two adjacent organic ligands on the surface of the NCs (i.e., dimerization).

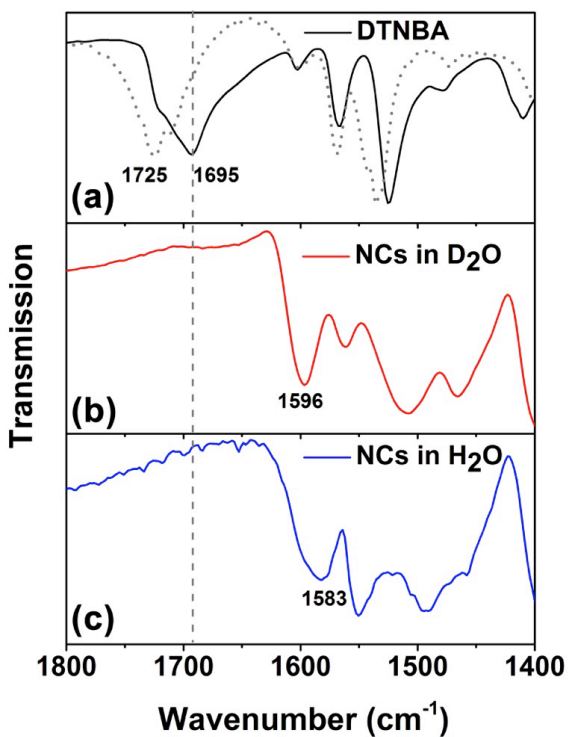


Figure 2. FTIR spectra of (a) pure capping ligands in powder form (solid curve) and in MeOH (dotted curve), (b) solid NCs prepared from protonated deuterated water and (c) solid NCs prepared from water.

Furthermore, the dimerization is also manifested through the changes of the C 1s core level peak structure. When Na^+ ion is present in the -carboxylate group (COONa^+), it makes both NO_2 and COOH moieties to “straighten up” and form the outmost layer of the ligand shell, which substantially shadows the benzene rings underneath. When Na^+ is replaced by H in the carboxylic group, i.e.

dimerization takes place between two adjacent ligands, resulting in the tilt of carboxylates towards each other. Such an interaction will bring the two ligands closer to the metal core, and at the same time it exposes the benzene rings underneath causing significant attenuation of the COOH peak at BE 288.3 eV (Figure S2).

The modification of the COOH group also results in significant changes to the electronic structure. The complete electronic structure was studied by a combination of photoelectron spectroscopy (PES) and inverse photoelectron spectroscopy (IPES). The valence and conduction band (CB) structures are shown in Figure 3. The valence band of deprotonated $\text{Ag}_{44}(\text{MNBA})_{30}$ NCs is comprised of three spectral features located at -2.2 eV , -4 eV , and -5.6 eV with the valence band maximum at -5.5 eV . The conduction band consists of four spectral features centered around -1 eV , -2.6 eV , -4.5 eV and -5.5 eV . The electronic band gap is estimated to be 1.35 eV , while the valence band maximum (VBM) positioned at -0.45 eV and conduction band minimum (CBM) at 0.9 eV above the Fermi level, as plotted in Figure 3, and thus in a good agreement with the optical measurements.

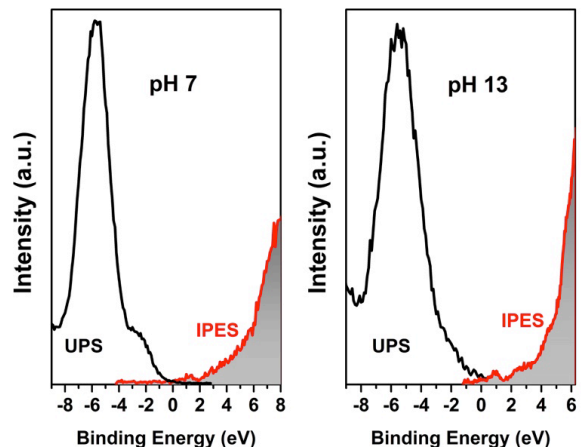


Figure 3. UPS/IPES spectra of Ag_{44} NCs thin films deposited from solutions of different pH. All binding energies are denoted at $E-E_F$, making occupied state binding energies negative.

A slightly larger band gap (BG) value with the combination of photoemission and inverse photoemission is expected and is due to the fundamental differences between optical absorption and the electronic spectroscopy. Photoemission and inverse photoemission are final state spectroscopies that, in the absence of full screening, lead to an apparent increase in the measured gap to a value greater than the ground state HOMO-LUMO gap (depending on the final state screening)⁴⁰, even in

molecular systems.^{41, 42} On the other hand, the optical absorption measurements may result in a smaller value than the actual ground state HOMO-LUMO gap because the optical excitation leaves a hole that, through Columbic interaction, leaves the measurement smaller than the ground state gap.⁴³ The small feature at the conduction band minimum, seen in Figure 3, is very similar to the surface state feature associated with clean silver surfaces, and is certainly consistent with the unoccupied state related to the coinage metals (Cu, Ag, Au).⁴⁴

When Na in the COONa⁺ group is replaced by H, significant changes in the electronic structure are observed. The valence band is now comprised of two spectral features located at -2.5 eV and -5.6 eV with the valence band maximum at -5.7 eV and a significantly sharper band edge. The features in the conduction band become less pronounced, shifted to higher energies (2.3 eV, and 3.5 eV) and in some cases cannot be identified. There is a tendency for the *band gap to widen by about 0.7 eV* and band gap value is estimated to be about 2.0 eV. This is consistent with the optical measurements, suggesting that this is not simply a ligand effect, affecting only the surface of the colloidal silver quantum dot. The energy shifts here, in inverse photoemission, are *ca* 0.5 eV and in the optical spectroscopy they are estimated to be around 100-200 meV, so that the energy shifts in the optical transition are less than the unoccupied band state shifts suggested by inverse photoemission. This does suggest that the surface or ligand envelope is a significant contribution to the charges in the inverse photoemission spectroscopy, which is more surface sensitive than the optical spectroscopy. The peak around 1 eV in the Ag NC's COONa⁺ sample closely resembles the expected Ag_{5s}-Ag_{4d} hybrid band and suggests that this is a more "metallic" NC than the COOH.

Transient-absorption measurements provide additional evidence for the modified electronic structure of the clusters as Na⁺ is substituted with H. Our previous transient-absorption measurements, on clusters with 4-fluorothiophenol, 2-naphthalenethiol, or 4-mercaptobenzoic acid, showed that excitation of the clusters with a laser pulse results in ultrafast charge separation followed by slow charge recombination.⁴⁵ In these more recent samples, with COONa⁺, the transient absorption spectra measured using ultrafast systems Helios (experimental details described elsewhere)⁴⁶ that are very similar to those prior results,⁴⁵ as shown in Figure 4 (bottom panel). The TA spectra show ground-state bleach (GSB) at 400 nm and 480 nm corresponding to peaks in the steady-state absorption spectra, and excited-state absorption (ESA) bands, which appears at 450 nm, 532 nm and

612 nm. As can be seen, the GSB signals are partially recovered within 5.5 ns time delay and ESA band decays up to 90% due to the charge recombination. The decay at both GSB and ESA is described by two time constants: an ultrafast decay time of picosecond, corresponding to charge separation, and a slow decay time of approximately 2 ns, corresponding to charge recombination. Both of these time constants are comparable to those previously observed for clusters in water.⁴⁵

For the COOH sample, in contrast, upper panel of Figure 4 shows that the transient spectra are dominated by a single bleach feature, at a wavelength corresponding to the single peak within the UV spectral region. It is observed that within 5.44 ns time delay, GSB is partially recovered and ESA band decays up to only 70% corresponding to charge recombination, which is slower compared to deprotonated cluster.

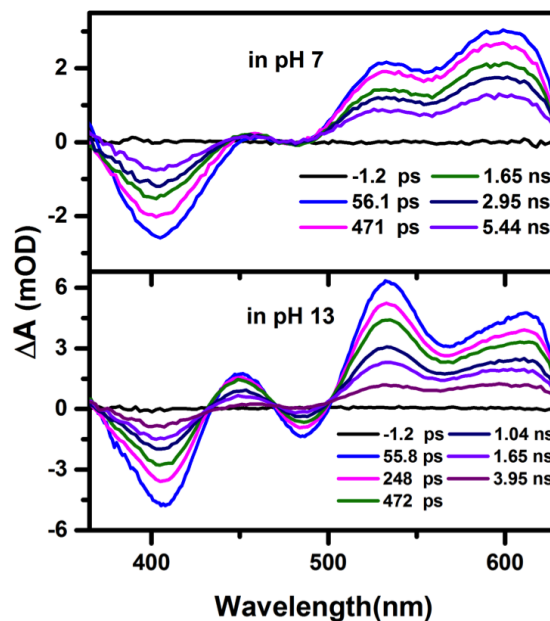


Figure 4. Femtosecond transient absorption spectra for Ag₄₄ NCs in pH 7 (top) and in pH 13 (bottom), using photoexcitation at 350 nm.

The change in the carrier dynamics at different pH is consistent with the change in electronic structure inferred from the linear absorption, PES, and IPES spectra. As stated above, substituting Na⁺ with H increases the energy level for separation in the cluster, increasing the difference in free energy between the initial and final states for charge separation, and leading to slower carrier dynamics especially charge recombination. To further support this interpretation, we repeated the transient-absorption measurements on solutions with a series

of pH values. The charge separation and recombination times were obtained by global fitting of the time-dependent transient spectra. Results are summarized in Figure 5. Both time constants vary exponentially with pH; this would be consistent with charge separation in the normal Marcus regime, if the free-energy difference for charge separation depends linearly on pH. Finally, the pH dependence of charge separation and recombination times may also be partially due to changes in the overlap between initial and final electronic wave functions as the conformational state of the ligands is changed.

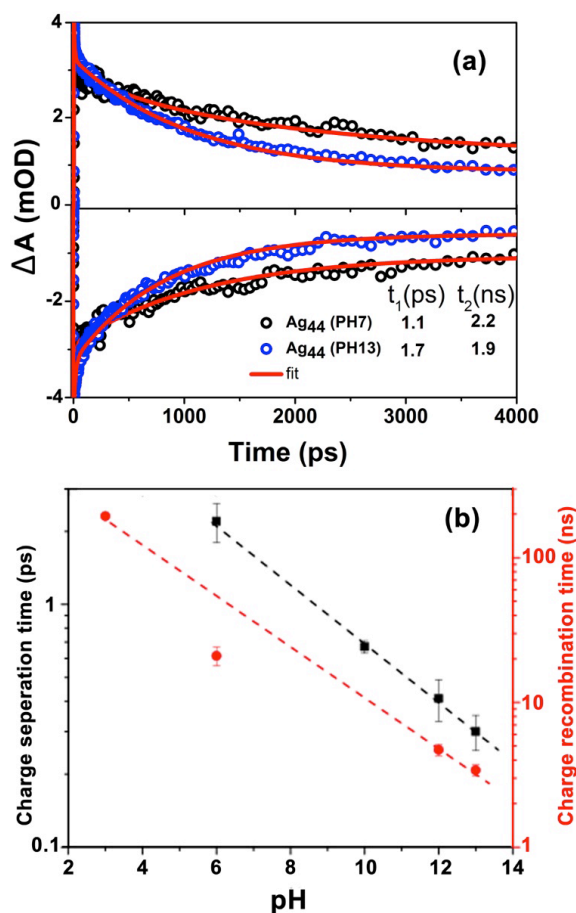


Figure 5. Femtosecond kinetic traces of Ag_{44} at ESA (top) and at GSB (bottom), using photoexcitation at 350 nm. (b) Fitted charge separation and recombination times for clusters in aqueous solution with different pH. The dashed lines are there as a guide only.

Conclusion

In summary, we report, for the first time, a new approach to tune both the optical and electronic properties of monodisperse thiol-protected silver

$\text{Ag}_{44}(\text{MNBA})_{30}$ NCs, by simply controlling the pH of the ligand shell. The changes in the optical and electronic properties have been confirmed by a combination of steady-state and femtosecond time resolved experiments. Interestingly, our results demonstrate that a dimerization between two adjacent ligands capping the NCs takes place upon changing the pH from 13 to 7. We believe that the novel insights reported in this work provide a fundamental understanding of the key variables involved in silver nanoclusters engineering, thus paving the way towards their exploitation for precise control of electronic structure and photo-physics of nanoclusters in general.

ASSOCIATED CONTENT

Supporting Information. The Supporting Information is available free of charge on the ACS Publications website.

AUTHOR INFORMATION

Corresponding Author

* katsievk@sabic.com

* omar.abdelsaboar@kaust.edu.sa

Author Contributions

The manuscript was written through contributions of all authors. All authors have given approval to the final version of the manuscript.

ACKNOWLEDGMENT

The measurements at Nebraska were partly supported by the U.S. Department of Energy through grant #DE-FG02-07ER15842 and the Nebraska Center for Energy Sciences Research.

REFERENCES

- (1) Dubois, F.; Mahler, B.; Dubertret, B.; Doris, E.; Mioskowski, C., A versatile strategy for quantum dot ligand exchange. *J. Am. Chem. Soc.* **2007**, 129, 482-483.
- (2) Wang, X.; Tilley, R. D.; Watkins, J. J., Simple Ligand Exchange Reactions Enabling Excellent Dispersibility and Stability of Magnetic Nanoparticles in Polar Organic, Aromatic, and Protic Solvents. *Langmuir* **2014**, 30, 1514-1521.
- (3) Brown, L. O.; Hutchison, J. E., Controlled growth of gold nanoparticles during ligand exchange. *J. Am. Chem. Soc.* **1999**, 121, 882-883.
- (4) Ling, D.; Hackett, M. J.; Hyeon, T., Surface ligands in synthesis, modification, assembly and biomedical applications of nanoparticles. *Nano Today* **2014**, 9, 457-477.

- (5) MbnhgnKonstantatos, G.; Howard, I.; Fischer, A.; Hoogland, S.; Clifford, J.; Klem, E.; Levina, L.; Sargent, E. H., Ultrasensitive solution-cast quantum dot photodetectors. *Nature* **2006**, 442, 180-183.
- (6) Kovalenko, M. V.; Scheele, M.; Talapin, D. V., Colloidal nanocrystals with molecular metal chalcogenide surface ligands. *Science* **2009**, 324, 1417-1420.
- (7) Huynh, W. U.; Dittmer, J. J.; Alivisatos, A. P., Hybrid nanorod-polymer solar cells. *Science* **2002**, 295, 2425-2427.
- (8) Kovalenko, M. V.; Schaller, R. D.; Jarzab, D.; Loi, M. A.; Talapin, D. V., Inorganically Functionalized PbS-CdS Colloidal Nanocrystals: Integration into Amorphous Chalcogenide Glass and Luminescent Properties. *J. Am. Chem. Soc.* **2012**, 134, 2457-2460.
- (9) Nel, A. E.; Mädler, L.; Velegol, D.; Xia, T.; Hoek, E. M.; Somasundaran, P.; Klaessig, F.; Castranova, V.; Thompson, M., Understanding biophysicochemical interactions at the nano-bio interface. *Nat. Mater.* **2009**, 8, 543-557.
- (10) Kathiravan, A.; Renganathan, R., Effect of anchoring group on the photosensitization of colloidal TiO₂ nanoparticles with porphyrins. *J. Coll. and Inter. Sci.* **2009**, 331, 401-407.
- (11) Liu, J.; Alvarez, J.; Ong, W.; Román, E.; Kaifer, A. E., Phase transfer of hydrophilic, cyclodextrin-modified gold nanoparticles to chloroform solutions. *J. Am. Chem. Soc.* **2001**, 123, 11148-11154.
- (12) Whetten, R. L.; Khoury, J. T.; Alvarez, M. M.; Murthy, S.; Vezmar, I.; Wang, Z. L.; Stephens, P. W.; Cleveland, C. L.; Luedtke, W.; Landman, U., Nanocrystal gold molecules. *Adv. Mater.* **1996**, 8, 428-433.
- (13) Maity, P.; Xie, S.; Yamauchi, M.; Tsukuda, T., Stabilized gold clusters: from isolation toward controlled synthesis. *Nanoscale* **2012**, 4, 4027-4037.
- (14) Niihori, Y.; Matsuzaki, M.; Pradeep, T.; Negishi, Y., Separation of precise compositions of noble metal clusters protected with mixed ligands. *J. Am. Chem. Soc.* **2013**, 135, 4946-4949.
- (15) Jin, R.; Eah, S.-K.; Pei, Y., Quantum-sized metal nanoclusters. *Nanoscale* **2012**, 4, 4026-4026.
- (16) Tsukuda, T., Toward an atomic-level understanding of size-specific properties of protected and stabilized gold clusters. *Bull. Chem. Soc. of Jap.* **2012**, 85, 151-168.
- (17) Negishi, Y., Towards the Creation of Functionalized Metal Nanoclusters and Highly Active Photocatalytic Materials Using Thiolate-Protected Magic Gold Clusters. *Bull. Chem. Soc. of Jap.* **2014**, 87, 375-389.
- (18) Chen, S.; Ingram, R. S.; Hostetler, M. J.; Pietron, J. J.; Murray, R. W.; Schaaff, T. G.; Khoury, J. T.; Alvarez, M. M.; Whetten, R. L., Gold nanoelectrodes of varied size: transition to molecule-like charging. *Science* **1998**, 280, 2098-2101.
- (19) Walter, M.; Akola, J.; Lopez-Acevedo, O.; Jadzinsky, P. D.; Calero, G.; Ackerson, C. J.; Whetten, R. L.; Grönbeck, H.; Häkkinen, H., A unified view of ligand-protected gold clusters as superatom complexes. *Proc. Nat. Acad. of Sci.* **2008**, 105, 9157-9162.
- (20) Akola, J.; Walter, M.; Whetten, R. L.; Häkkinen, H.; Grönbeck, H., On the structure of thiolate-protected Au₂₅. *J. Am. Chem. Soc.* **2008**, 130, 3756-3757.
- (21) El-Ballouli, A. a. O.; Alarousu, E.; Bernardi, M.; Aly, S. M.; Lagrow, A. P.; Bakr, O. M.; Mohammed, O. F., Quantum Confinement-Tunable Ultrafast Charge Transfer at the PbS Quantum Dot and Phenyl-C61-butyric Acid Methyl Ester Interface. *J. Am. Chem. Soc.* **2014**, 136, 6952-6959.
- (22) Ahmed, G. H.; Aly, S. M.; Usman, A.; Eita, M. S.; Melnikov, V. A.; Mohammed, O. F., Quantum confinement-tunable intersystem crossing and the triplet state lifetime of cationic porphyrin-CdTe quantum dot nano-assemblies. *Chem. Commun.* **2015**, 51, 8010-8013.
- (23) Häkkinen, H.; Moseler, M., 55-Atom clusters of silver and gold: Symmetry breaking by relativistic effects. *Comp. Mater. Sci.* **2006**, 35, 332-336.
- (24) Beqa, L.; Deschamps, D.; Perrio, S.; Gaumont, A.-C.; Knoppe, S.; Bürgi, T., Ligand Exchange Reaction on Au₃₈ (SR)₂₄, Separation of Au₃₈ (SR)₂₃ (SR')₁ Regioisomers, and Migration of Thiolates. *J. of Phys. Chem. C* **2013**, 117, 21619-21625.
- (25) Dass, A.; Stevenson, A.; Dubay, G. R.; Tracy, J. B.; Murray, R. W., Nanoparticle MALDI-TOF mass spectrometry without fragmentation: Au₂₅ (SCH₂CH₂Ph)₁₈ and mixed monolayer Au₂₅ (SCH₂CH₂Ph)_{18-x} (L)_x. *J. Am. Chem. Soc.* **2008**, 130, 5940-5946.
- (26) Fields-Zinna, C. A.; Parker, J. F.; Murray, R. W., Mass Spectrometry of Ligand Exchange Chelation of the Nanoparticle [Au₂₅ (SCH₂CH₂C₆H₅)₁₈] ¹⁻ by CH₃C₆H₃ (SH)₂. *J. Am. Chem. Soc.* **2010**, 132, 17193-17198.
- (27) Hostetler, M. J.; Templeton, A. C.; Murray, R. W., Dynamics of place-exchange reactions on monolayer-protected gold cluster molecules. *Langmuir* **1999**, 15, 3782-3789.
- (28) Tracy, J. B.; Crowe, M. C.; Parker, J. F.; Hampe, O.; Fields-Zinna, C. A.; Dass, A.; Murray, R. W., Electrospray ionization mass spectrometry of uniform and mixed monolayer nanoparticles: Au₂₅ [S (CH₂)₂Ph]₁₈ and Au₂₅ [S (CH₂)₂Ph]_{18-x} (SR)_x. *J. Am. Chem. Soc.* **2007**, 129, 16209-16215.
- (29) Heimel, G.; Romaner, L.; Zojer, E.; Brédas, J.-L., Toward Control of the Metal-Organic Interfacial Electronic Structure in Molecular Electronics: A First-Principles Study on Self-Assembled Monolayers of π -Conjugated Molecules on Noble Metals. *Nano Lett.* **2007**, 7, 932-940.
- (30) Koch, N.; Gerlach, A.; Duhm, S.; Glowatzki, H.; Heimel, G.; Vollmer, A.; Sakamoto, Y.; Suzuki, T.; Zegenhagen, J.; Rabe, J. P.; Schreiber, F., Adsorption-Induced Intramolecular Dipole: Correlating Molecular Conformation and Interface Electronic Structure. *J. Am. Chem. Soc.* **2008**, 130, 7300-7304.

- (31) Rissner, F.; Egger, D. A.; Romaner, L.; Heimel, G.; Zojer, E., The Electronic Structure of Mixed Self Assembled Monolayers. *ACS Nano* **2010**, 4, 6735-6746.
- (32) Rissner, F.; Rangger, G. M.; Hofmann, O. T.; Track, A. M.; Heimel, G.; Zojer, E., Understanding the Electronic Structure of Metal/SAM/Organic-Semiconductor Heterojunctions. *ACS Nano* **2009**, 3, 3513-3520.
- (33) Aikens, C. M., Electronic Structure of Ligand-Passivated Gold and Silver Nanoclusters. *J. of Phys. Chem. Lett.* **2011**, 2, 99-104.
- (34) AbdulHalim, L. G.; Ashraf, S.; Katsiev, K.; Kirmani, A. R.; Kothalawala, N.; Anjum, D. H.; Abbas, S.; Amassian, A.; Stellacci, F.; Dass, A.; Hussain, I.; Bakr, O. M., A scalable synthesis of highly stable and water dispersible Ag₄₄ (SR)₃₀ nanoclusters. *J. Mater. Chem. A* **2013**, 1, 10148-10154.
- (35) Kamei, Y.; Robertson, N.; Shichibu, Y.; Konishi, K., Impact of Skeletal Isomerization of Ultrasmall Gold Clusters on Electrochemical Properties: Voltammetric Profiles of Nonspoked Octanuclear Clusters. *J. Phys. Chem. C* **2015**, 119, 10995-10999.
- (36) Gell, L.; Häkkinen, H., Theoretical Analysis of the M₁₂Ag₃₂(SR)₄₀₄⁻ and X@M₁₂Ag₃₂(SR)₃₀₄⁻ Nanoclusters (M = Au, Ag; X = H, Mn). *J. Phys. Chem. C* **2015**, 119, 10943-10948.
- (37) Tao, Y.; Dreger, Z. A.; Gupta, Y. M., High pressure effects on benzoic acid dimers: Vibrational spectroscopy. *Vib. Spec.* **2014**, 73, 138-143.
- (38) Tolstorozhev, G. B.; Bel'kov, M. V.; Skorniyakov, I. V.; Bazyl, O. K.; Artyukhov, V. Y.; Mayer, G. V.; Shadyro, O. I.; Kuzovkov, P. V.; Brinkevich, S. D.; Samovich, S. N., Infrared Spectroscopy of Hydrogen Bonds in Benzoic Acid Derivatives. *J. App. Spec.* **2014**, 81, 109-117.
- (39) Mohammed, O. F.; Kwon, O. H.; Othon, C. M.; Zewail, A. H., Charge Transfer Assisted by Collective Hydrogen-Bonding Dynamics. *Angew. Chem. Inter. Ed.* **2009**, 48, 6251-6256.
- (40) Ortega, J.; Himpsel, F.; Li, D.; Dowben, P., Initial and final state contributions of the core level shifts for Gd (0001). *Sol. St. Commun.* **1994**, 91, 807-811.
- (41) Cabellos, J. L.; Mowbray, D.; Goiri, E.; El-Sayed, A.; Floreano, L.; de Oteyza, D.; Rogero, C.; Ortega, J. E.; Rubio, A., Understanding Charge Transfer in Donor-Acceptor/Metal Systems: A Combined Theoretical and Experimental Study. *J. Phys. Chem. C* **2012**, 116, 17991-18001.
- (42) Xiao, J.; Dowben, P. A., The role of the interface in the electronic structure of adsorbed metal (II)(Co, Ni, Cu) phthalocyanines. *J. Mater. Chem.* **2009**, 19, 2172-2178.
- (43) Bredas, J.-L., Mind the gap! *Mater. Horiz.* **2014**, 1, 17-19.
- (44) Sundararaman, R.; Narang, P.; Jermyn, A. S.; Goddard Iii, W. A.; Atwater, H. A., Theoretical predictions for hot-carrier generation from surface plasmon decay. *Nat. Commun.* **2014**, 5.
- (45) Pelton, M.; Tang, Y.; Bakr, O. M.; Stellacci, F., Long-lived charge-separated states in ligand-stabilized silver clusters. *J. Am. Chem. Soc.* **2012**, 134, 11856-11859.
- (46) Bose, R.; Hamdi G.A.; Alarousu E.; Parida M. R.; Abdelhady A.L.; Bark O.M.; Mohammed O.F., Direct Femtosecond Observation of Charge Carrier Recombination in Ternary Semiconductor Nanocrystals: The Effect of Composition and Shelling. *J. Phys. Chem. C* **2015**, 119, 3439-3446.